

Supporting information

for

Synthesis, Characterization and Thermal Study of Divalent Germanium, Tin and Lead Triazenides as Potential Vapor Deposition Precursors

Rouzbeh Samii,^[a] David Zanders,^{[b],[c]} Anton Fransson,^[a] Goran Bačić,^[b] Sean T. Barry,^[b] Lars Ojamäe,^[a] Vadim Kessler,^[d] Henrik Pedersen,^[a] and Nathan J. O'Brien^{*,[a]}

^[a] Department of Physics, Chemistry and Biology, Linköping University, SE-581 83 Linköping, Sweden

^[b] Department of Chemistry, Carleton University, 1125 Colonel By Drive, Ottawa, Ontario, K1S5B6, Canada

^[c] Faculty of Chemistry and Biochemistry, Ruhr University Bochum, Universitätsstraße 150, 44801, Bochum, Germany

^[d] Department of Molecular Sciences, Swedish University of Agricultural Sciences, P.O. Box 7015, 75007 Uppsala, Sweden

*Corresponding author: nathan.o.brien@liu.se

Table of contents

NMR Spectra	S1-4
Thermogravimetric Analysis	S5-6
Differential Scanning Calorimetry	S7
EI-MS Data	S8
X-ray Crystallographic Analysis	S9-11
Computational Calculations	S12-13

NMR Spectra

^1H NMR (C_6D_6 , 300 MHz)
(1,3-di-*tert*-butyltriazene)Li(I)

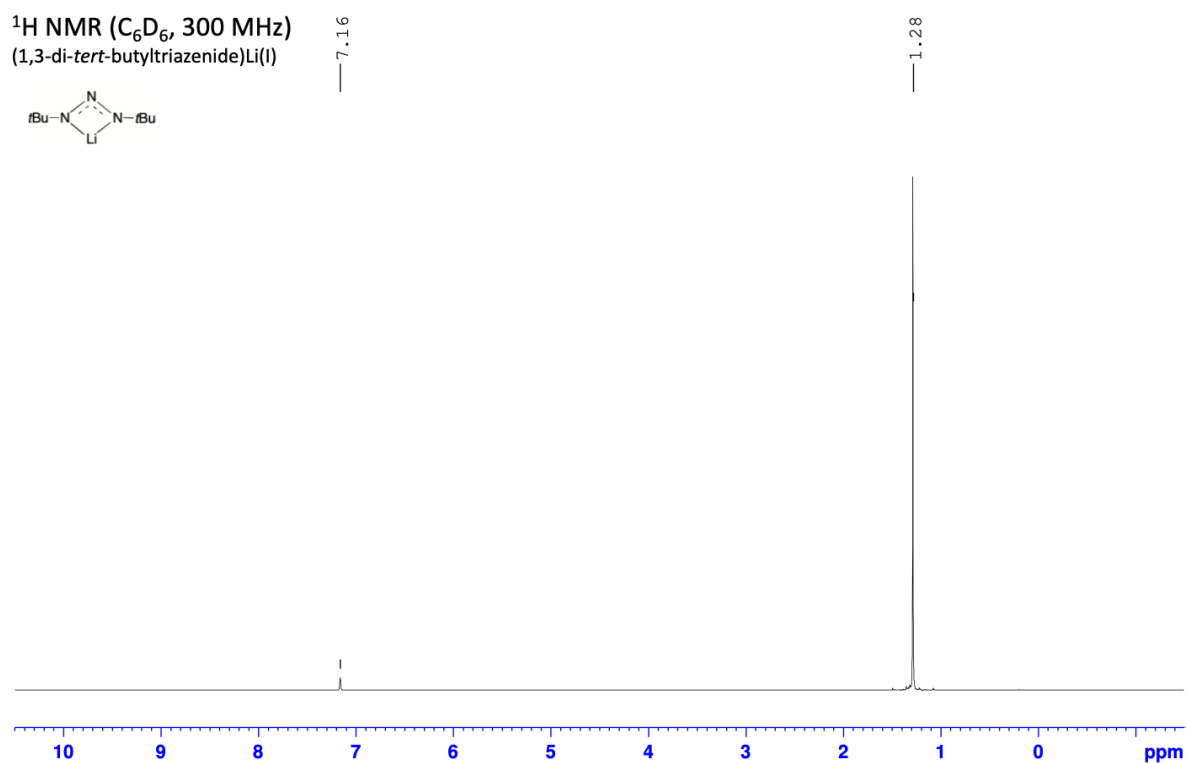
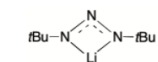


Figure S1: ^1H NMR (300 MHz) spectrum of (1,3-di-*tert*-butyltriazene)lithium(I) in C_6D_6 .

^{13}C NMR (C_6D_6 , 75 MHz)
(1,3-di-*tert*-butyltriazene)lithium(I)

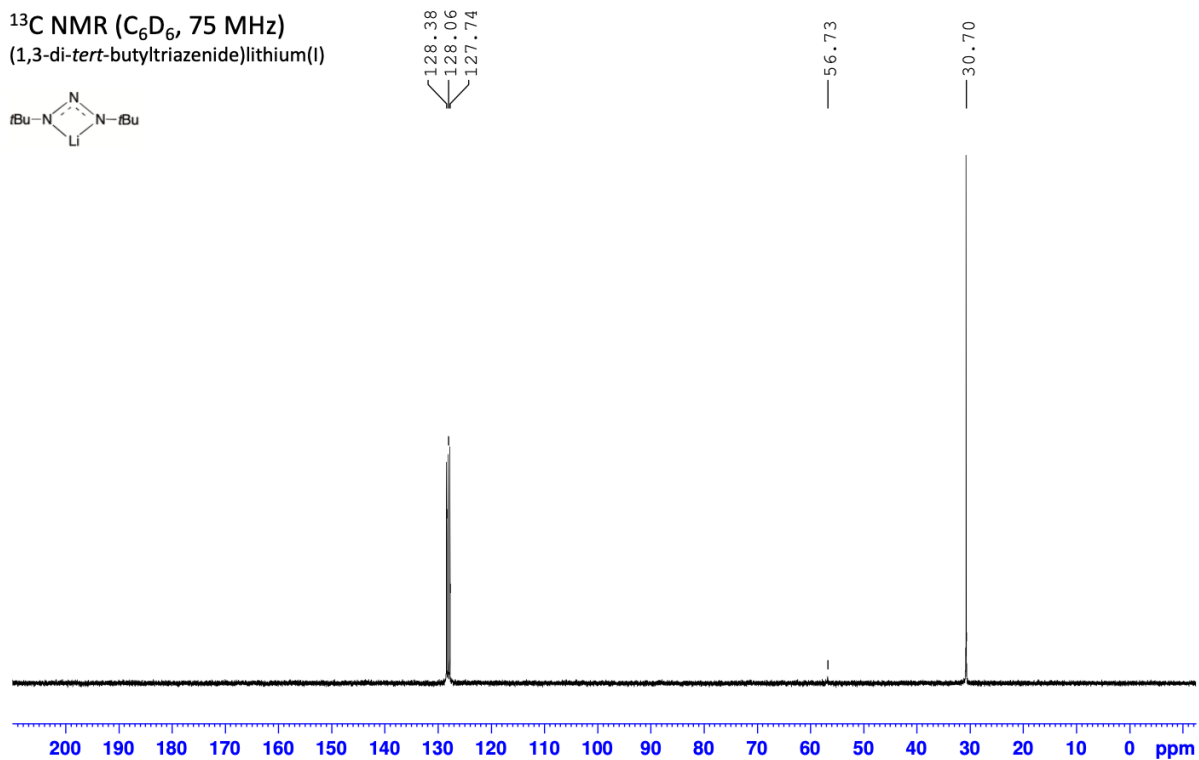
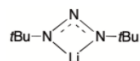


Figure S2: ^{13}C NMR (75 MHz) spectrum of (1,3-di-*tert*-butyltriazene)lithium(I) in C_6D_6 .

^1H NMR (C_6D_6 , 300 MHz)
Bis(1,3-di-*tert*-butyltriazene)germanium(II)

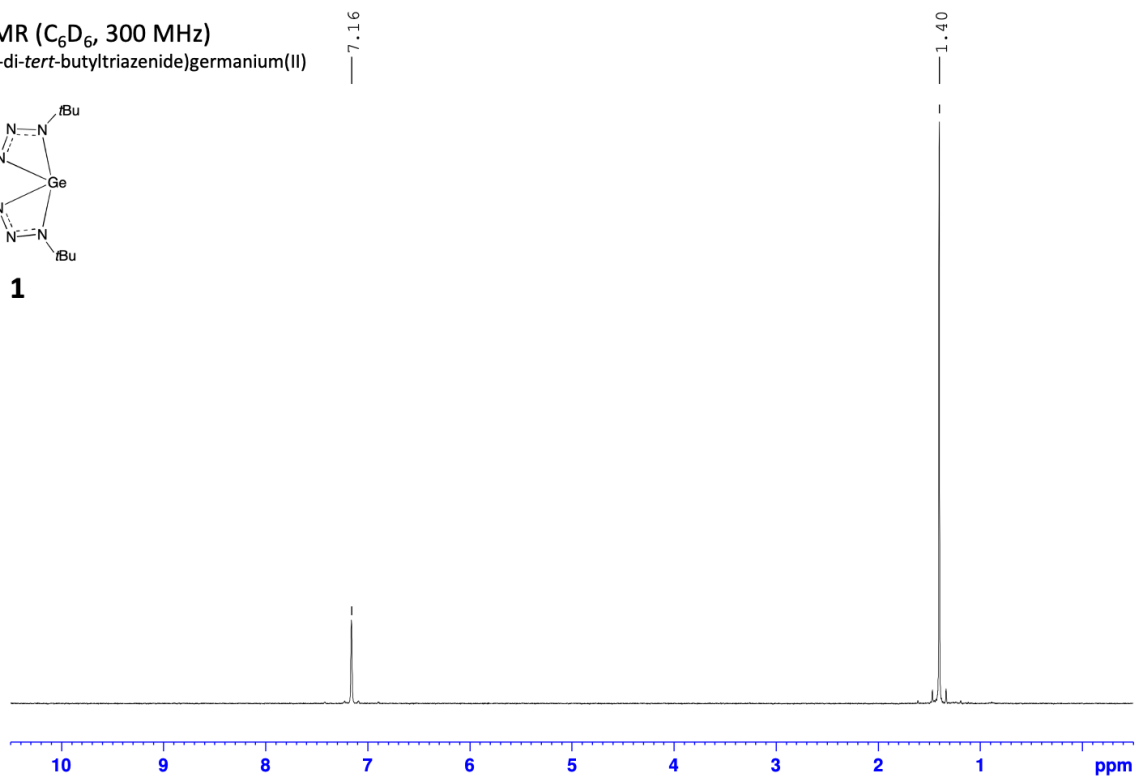
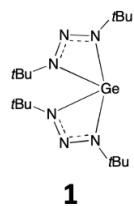


Figure S3: ^1H NMR (300 MHz) spectrum of **1** in C_6D_6 .

^{13}C NMR (C_6D_6 , 125 MHz)
Bis(1,3-di-*tert*-butyltriazene)germanium(II)

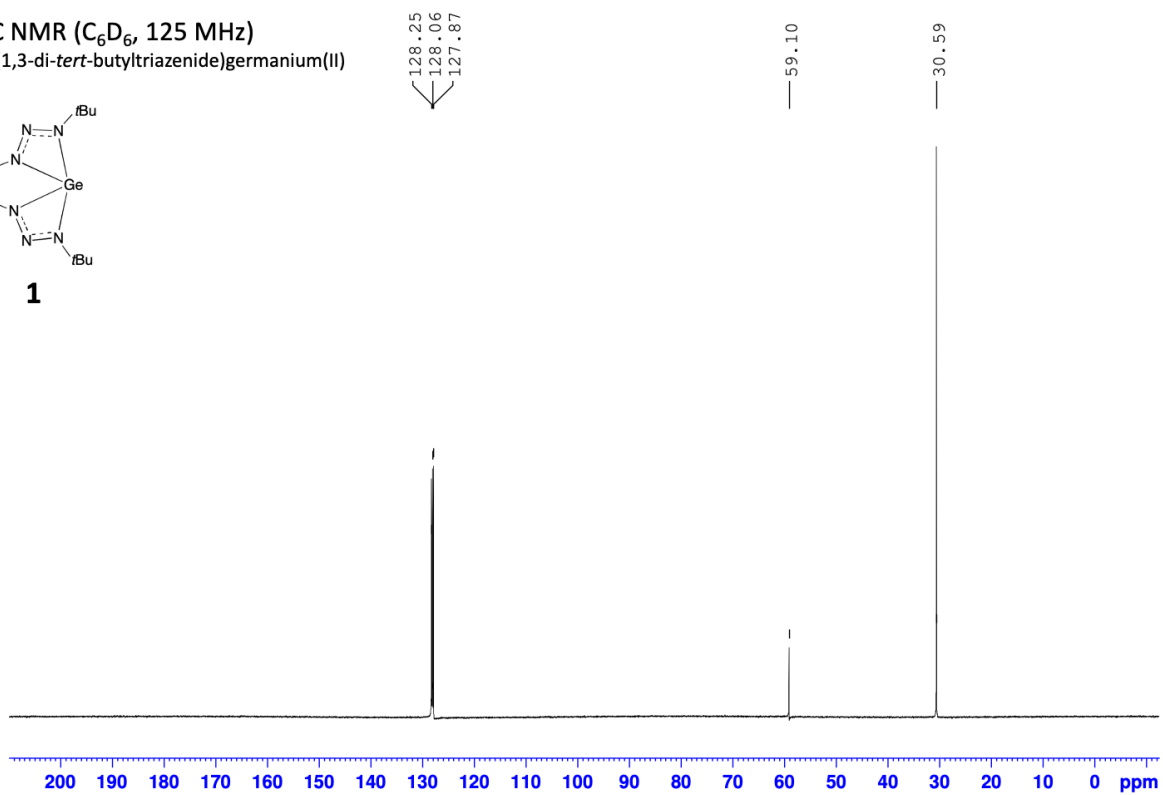
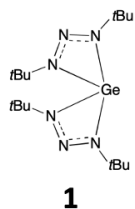


Figure S4: ^{13}C NMR (125 MHz) spectrum of **1** in C_6D_6 .

^1H NMR (C_6D_6 , 500 MHz)
Bis(1,3-di-*tert*-butyltriazene)tin(II)

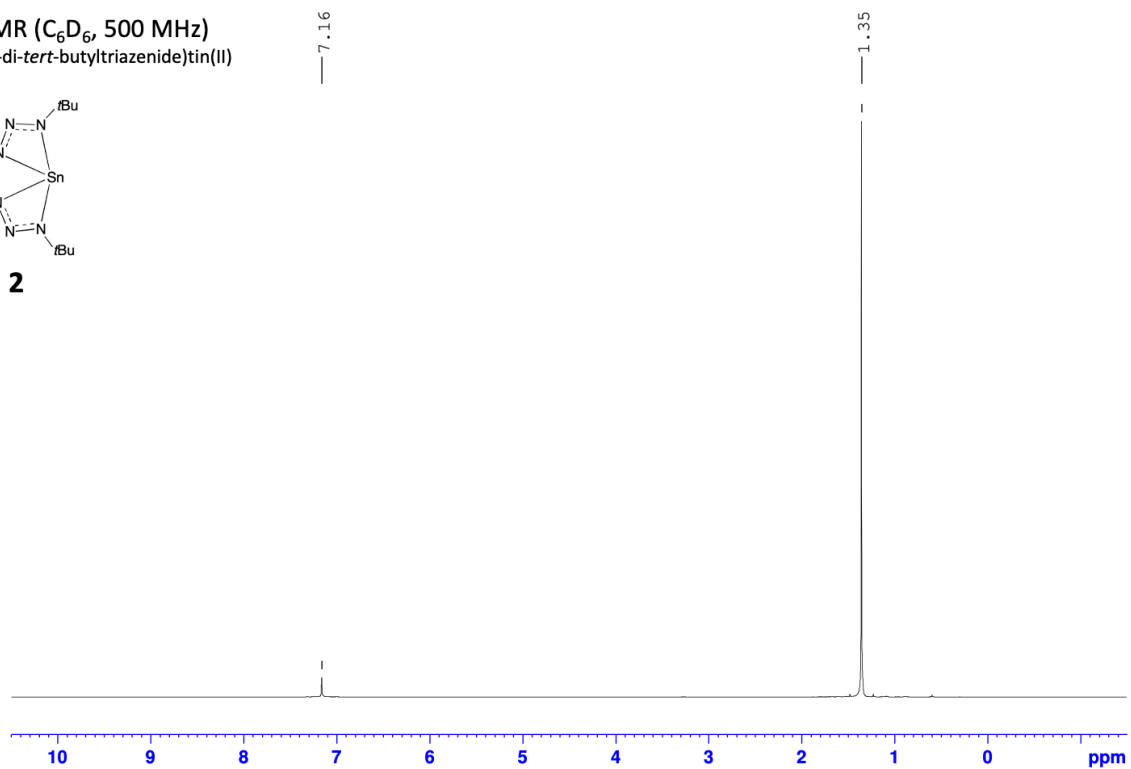
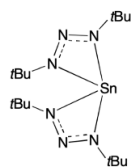


Figure S5: ^1H NMR (500 MHz) spectrum of **2** in C_6D_6 .

^{13}C NMR (C_6D_6 , 125 MHz)
Bis(1,3-di-*tert*-butyltriazene)tin(II)

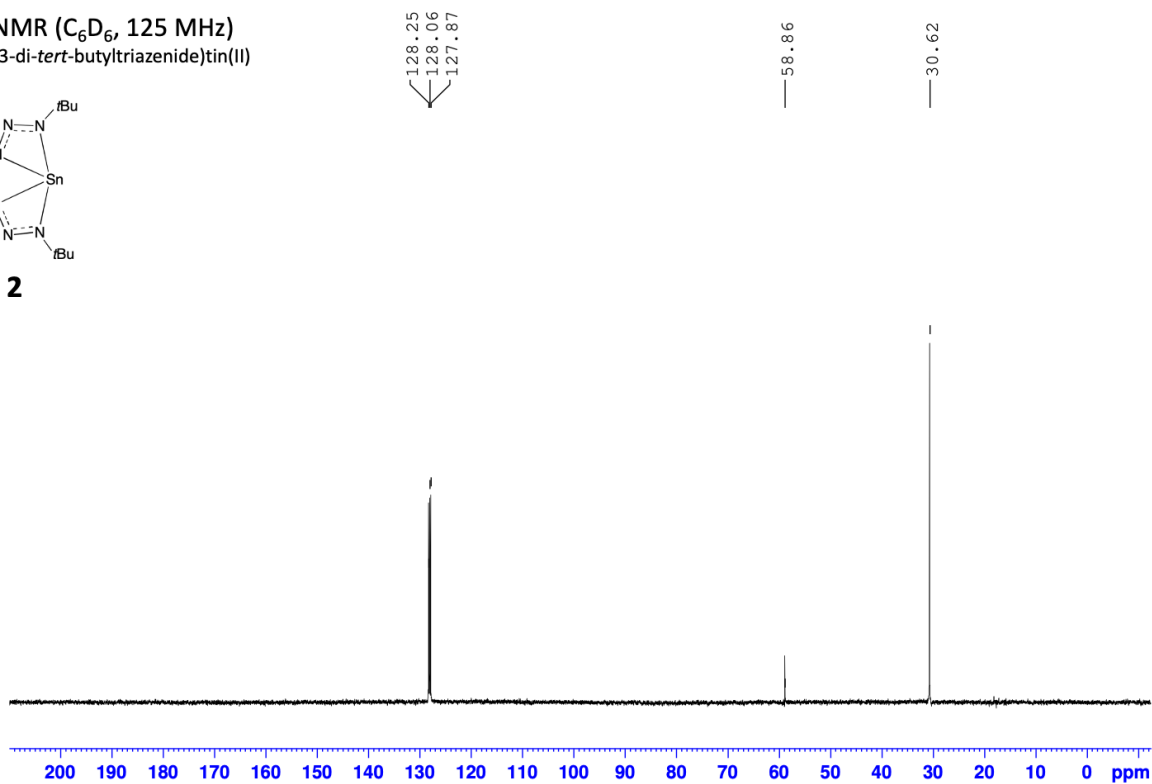
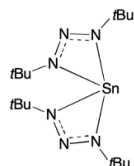


Figure S6: ^{13}C NMR (125 MHz) spectrum of **2** in C_6D_6 .

^1H NMR (C_6D_6 , 500 MHz)
Bis(1,3-di-*tert*-butyltriazene)lead(II)

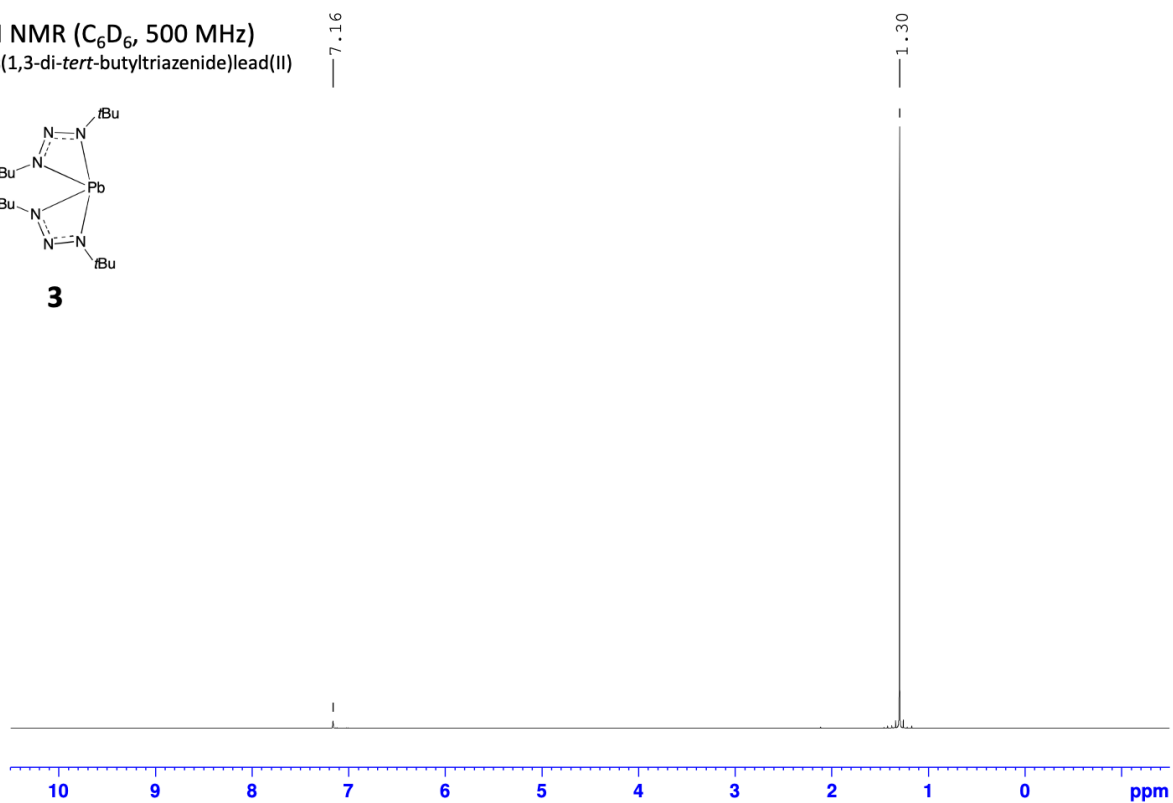
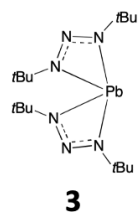


Figure S7: ^1H NMR (500 MHz) spectrum of **3** in C_6D_6 .

^{13}C NMR (C_6D_6 , 125 MHz)
Bis(1,3-di-*tert*-butyltriazene)lead(II)

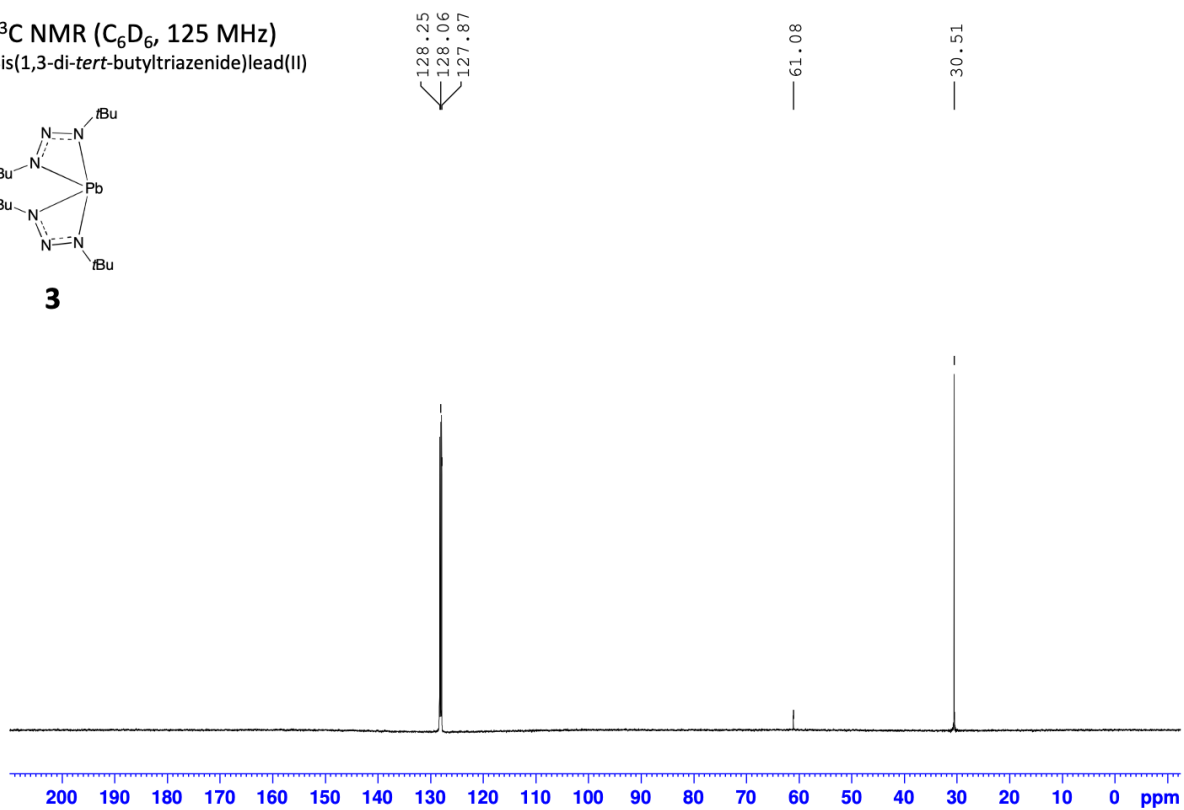
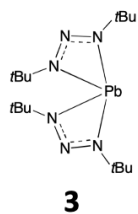


Figure S8: ^{13}C NMR (125 MHz) spectrum of **3** in C_6D_6 .

Thermogravimetric Analysis

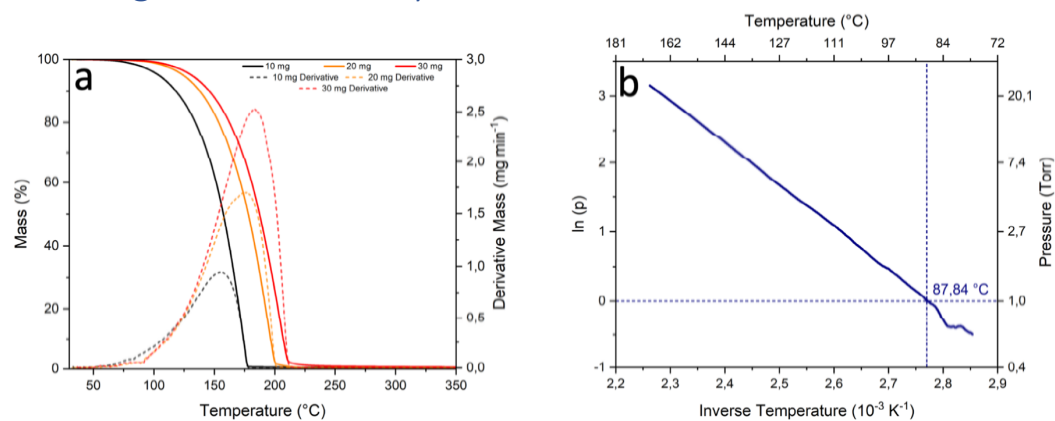


Figure S9: TGA of **1** (a) and Clausius-Clapeyron plot of **1** for derived from TGA data using 10 mg sample size (b).

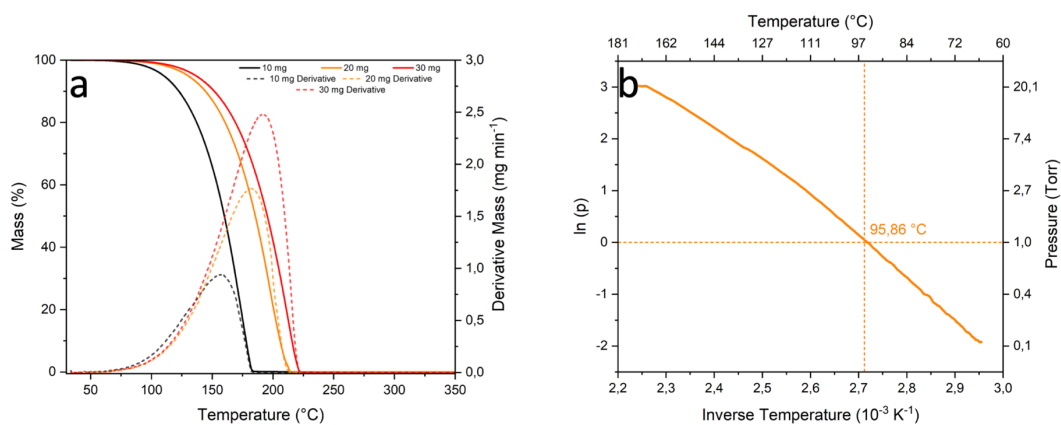


Figure S10: TGA of **2** (a) and Clausius-Clapeyron plot of **1** for derived from TGA data using 10 mg sample size (b).

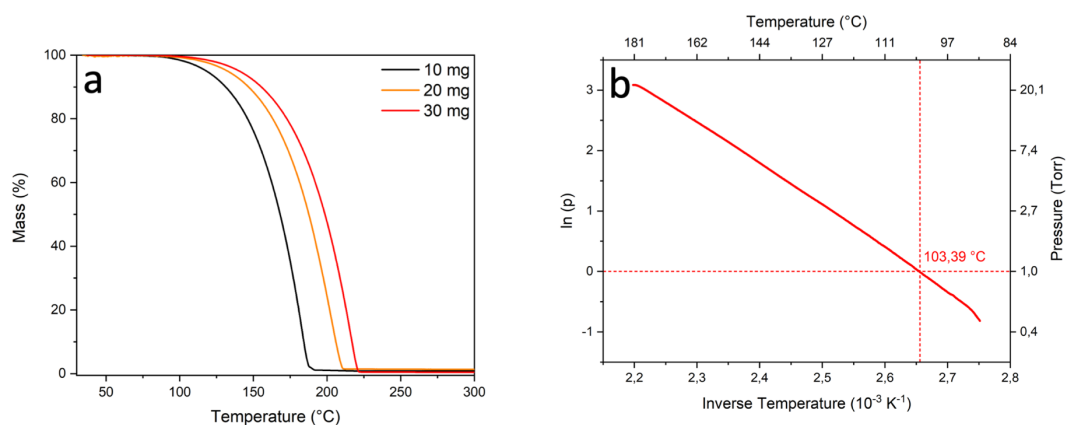


Figure S11: TGA of **3** (a) and Clausius-Clapeyron plot of **1** for derived from TGA data using 10 mg sample size (b).

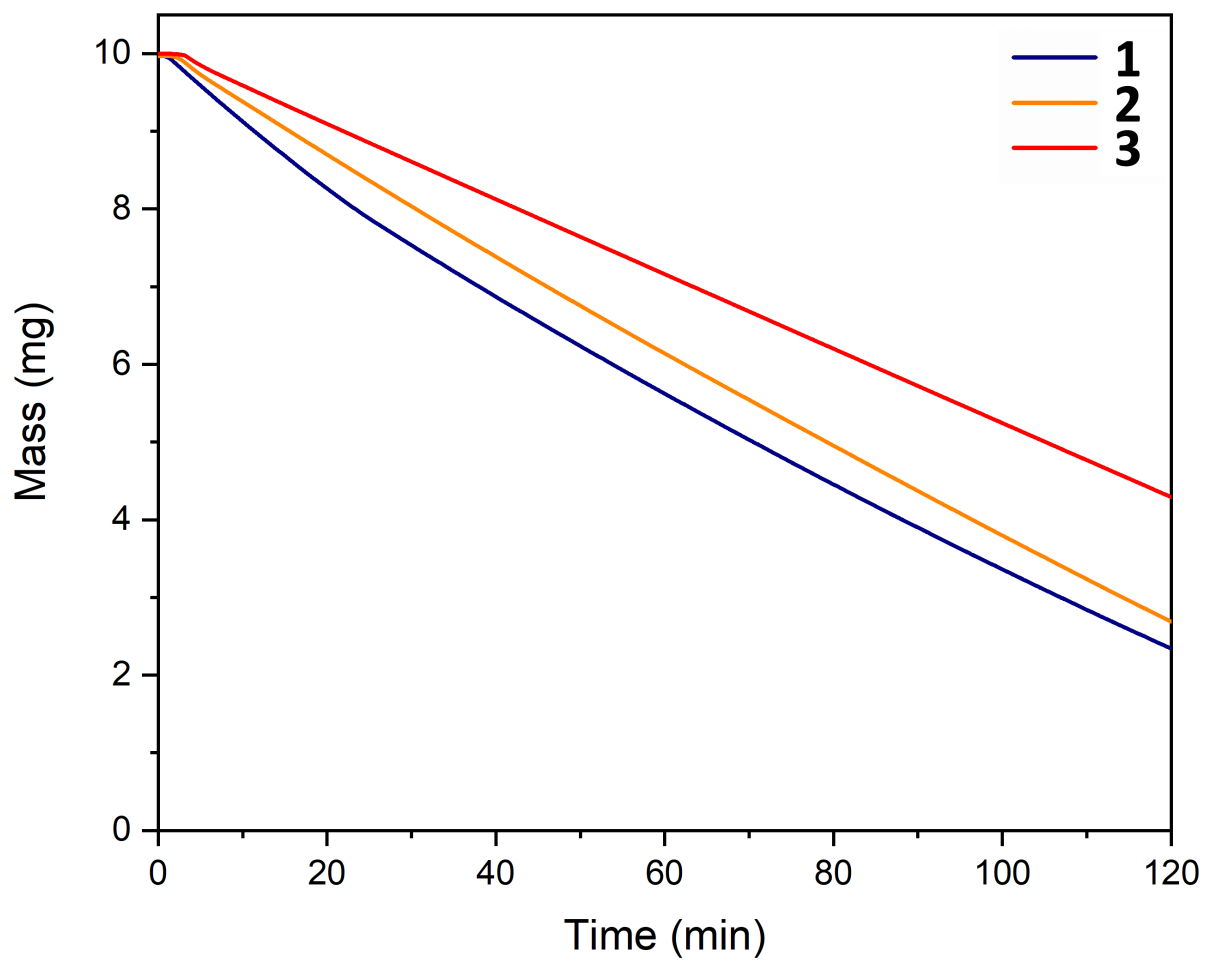


Figure S12: Isothermal TGA of **1–3** at 90 °C.

Differential Scanning Calorimetry

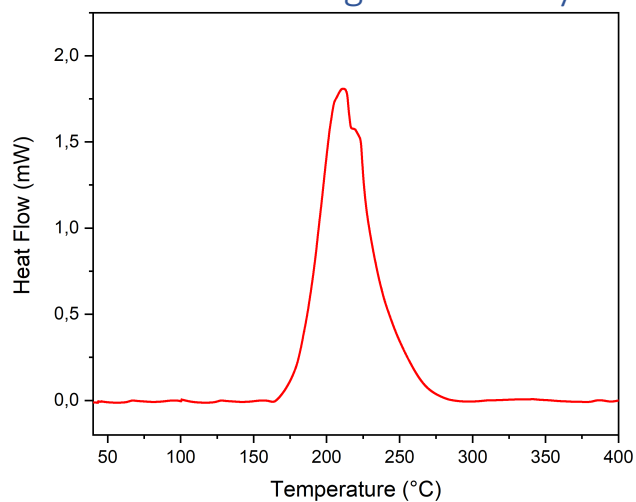


Figure S13: Base line corrected DSC of **1**.

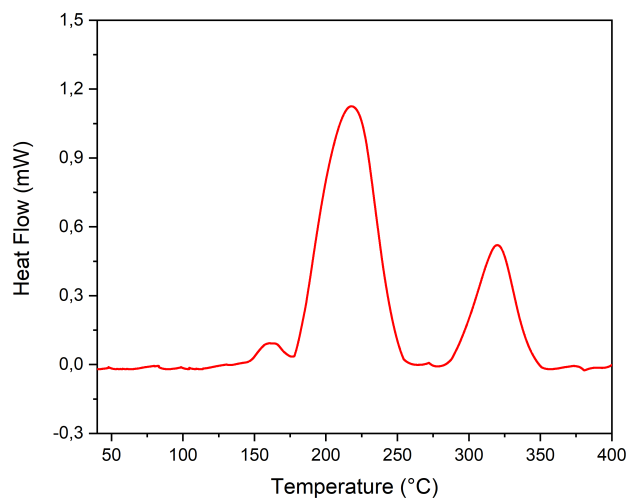


Figure S14: Base line corrected DSC of **2**.

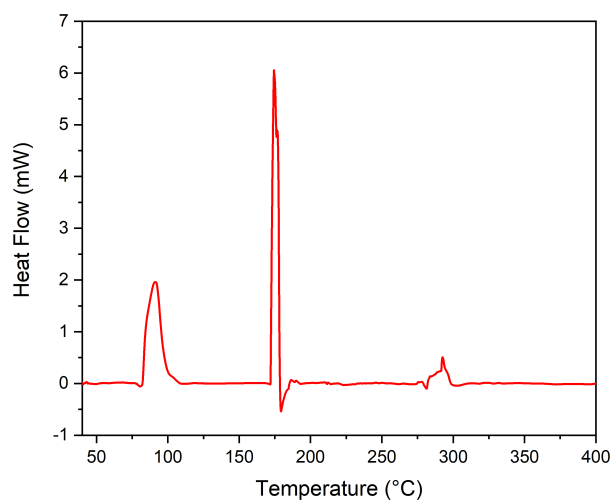


Figure S15: Base line corrected DSC of **3**.

EI-MS Data

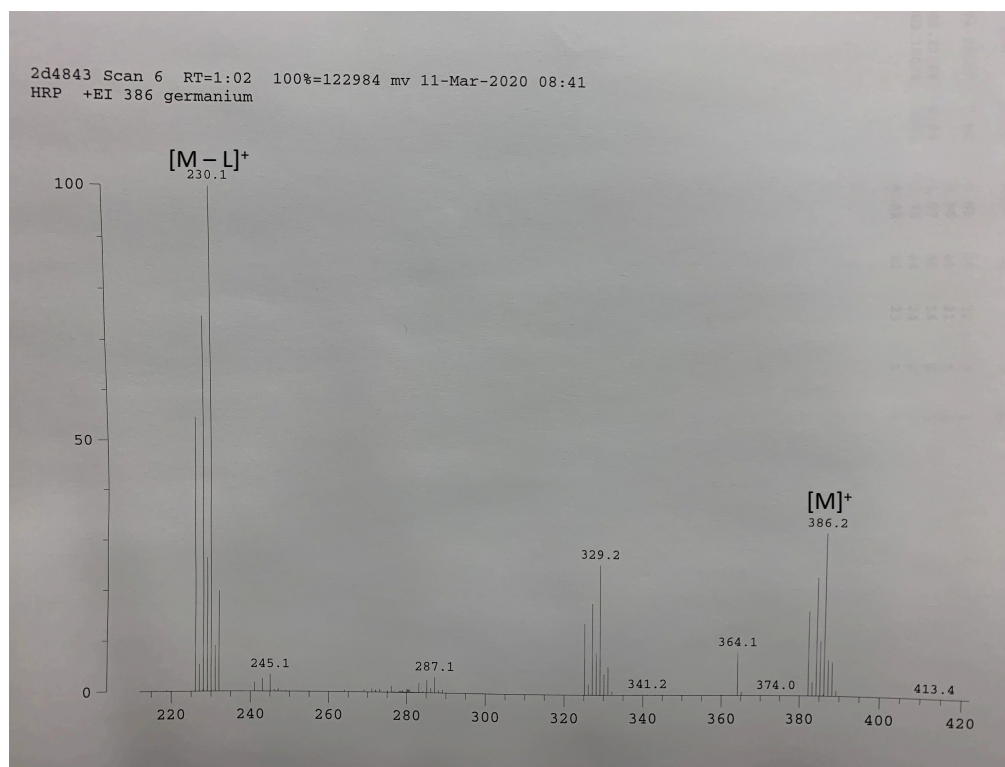


Figure S16: EI-MS of **1**.

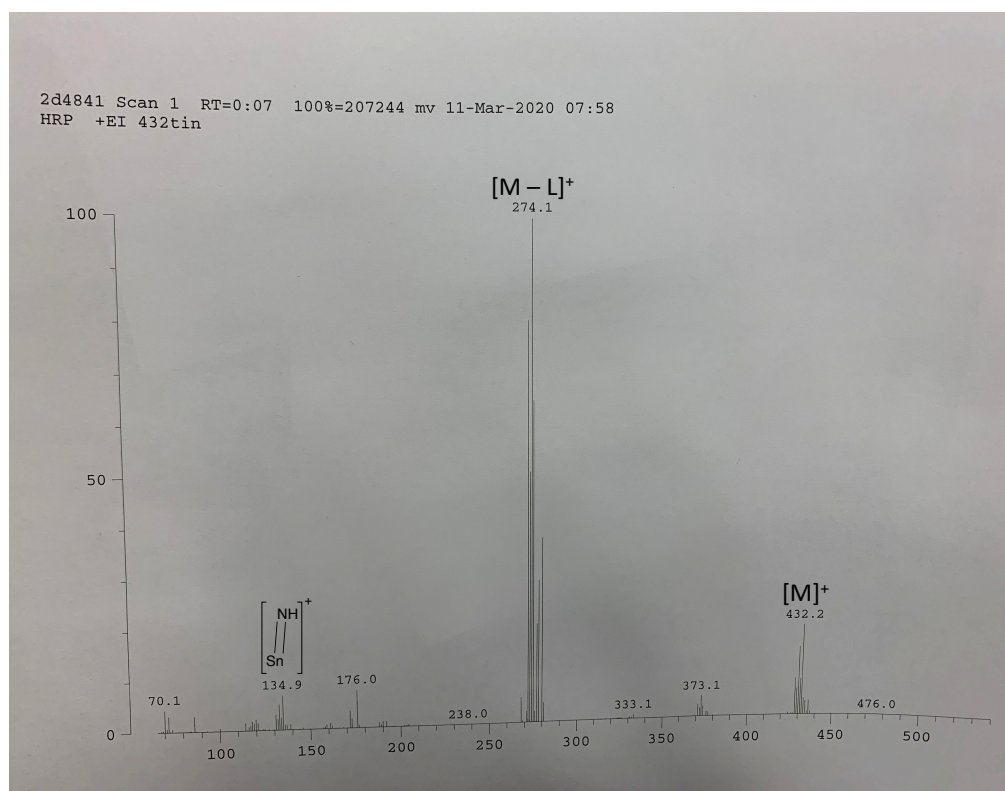


Figure S17: EI-MS of **2**.

X-ray Crystallographic Analysis

Table S1: Bond lengths (Å) and bond angles (°) for **1** from structure determination by X-ray crystallography and quantum chemical DFT calculations.

	XRD	DFT
Ge1–N1	1.995	2.036
Ge1–N2	2.217	2.276
N1–N3	1.310	1.297
N2–N3	1.301	1.280
N1–C1	1.477	1.478
N2–C2	1.479	1.482
N1–Ge1–N1	98.15	96.48
N1–Ge1–N2 inter	98.25	94.77
N1–Ge1–N2 intra	59.64	58.24
N2–Ge1–N2	147.92	141.12
N1–N3–N2	107.35	109.54

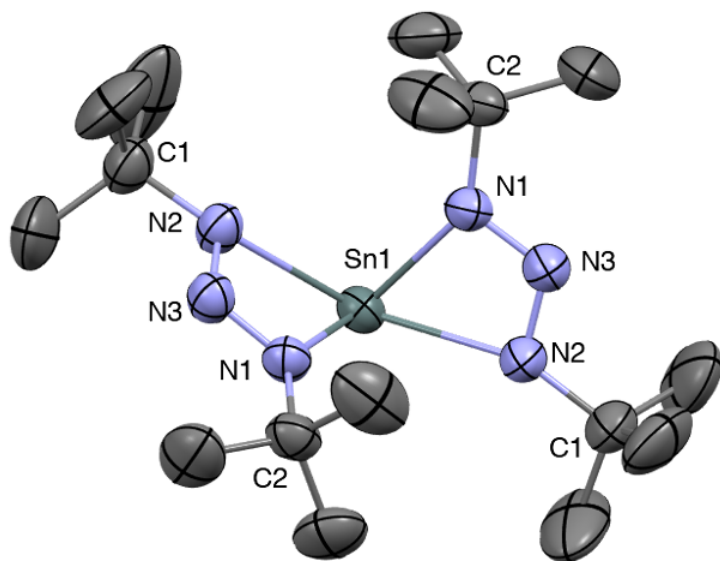


Figure S18: Crystal structure of **2**, thermal ellipsoids are depicted at 50% probability level and all hydrogens were removed for clarity.

Table S2: Bond lengths (Å) and bond angles (°) for **2** from structure determination by X-ray crystallography and quantum chemical DFT calculations.

	XRD	DFT
Sn1–N2	2.207	2.248

Sn1–N3	2.388	2.423
N1–N2	1.295	1.291
N1–N3	1.293	1.280
N2–C2	1.486	1.475
N3–C1	1.471	1.479
N2–Sn1–N2	93.99	92.18
N3–Sn1–N3	133.39	131.31
N2–Sn1–N3_inter	92.05	90.91
N2–Sn1–N3_intra	54.87	54.02
N2–N1–N3	110.27	111.59

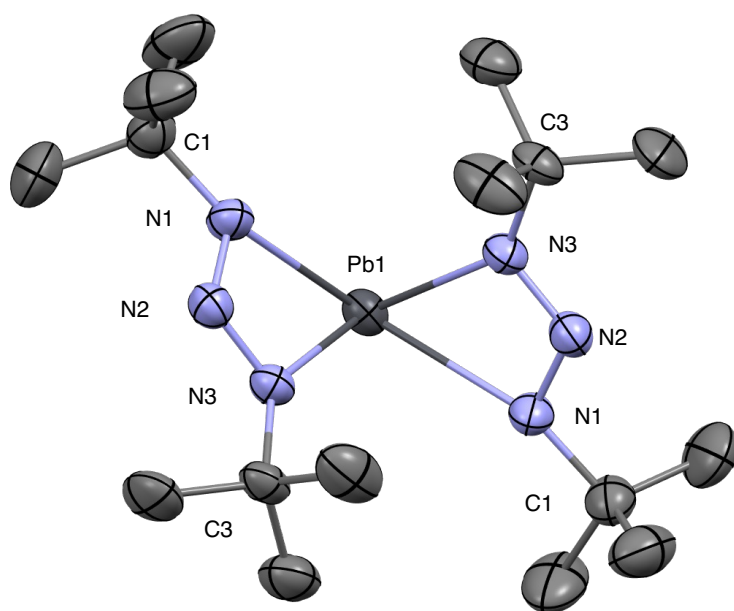


Figure S19: Crystal structure of **3**, thermal ellipsoids are depicted at 50% probability level and all hydrogens were removed for clarity.

Table S3: Bond lengths (Å) and bond angles (°) for **3** from structure determination by X-ray crystallography and quantum chemical DFT calculations.

	XRD	DFT
Pb1–N1	2.503	2.423
Pb1–N3	2.328	2.248
N1–N2	1.292	1.291
N2–N3	1.291	1.280
N1–C1	1.476	1.475

N3–C3	1.472	1.479
N1–Pb1–N1	129.61	131.31
N3–Pb1–N3	92.13	92.18
N1–Pb1–N3_inter	91.01	90.91
N1–Pb1–N3_intra	52.54	54.02
N1–N2–N3	112.21	111.59

Geometry index, τ'_4 , is defined as:

$$\tau'_4 = \frac{\beta - \alpha}{360^\circ - 109.5^\circ} + \frac{180^\circ - \beta}{180^\circ - 109.5^\circ},$$

where α and β are the two widest N–M–N angles and $\beta > \alpha$. For compound **1**, the widest angles are 98.25 and 147.92° (Table S1). Substituting α and β for 98.25 and 147.92°, respectively in the equation for calculating τ'_4 gives:

$$\tau'_4 = \frac{147.92 - 98.25}{360^\circ - 109.5^\circ} + \frac{180^\circ - 147.92}{180^\circ - 109.5^\circ} \approx 0.65.$$

Similar calculations for compound **2** using $\alpha = 93.99^\circ$ and $\beta = 133.39^\circ$ (Table S2) yields $\tau'_4 = 0.82$, and for compound **3** using $\alpha = 92.13^\circ$ and $\beta = 129.61^\circ$ (Table S3) yields $\tau'_4 = 0.86$.

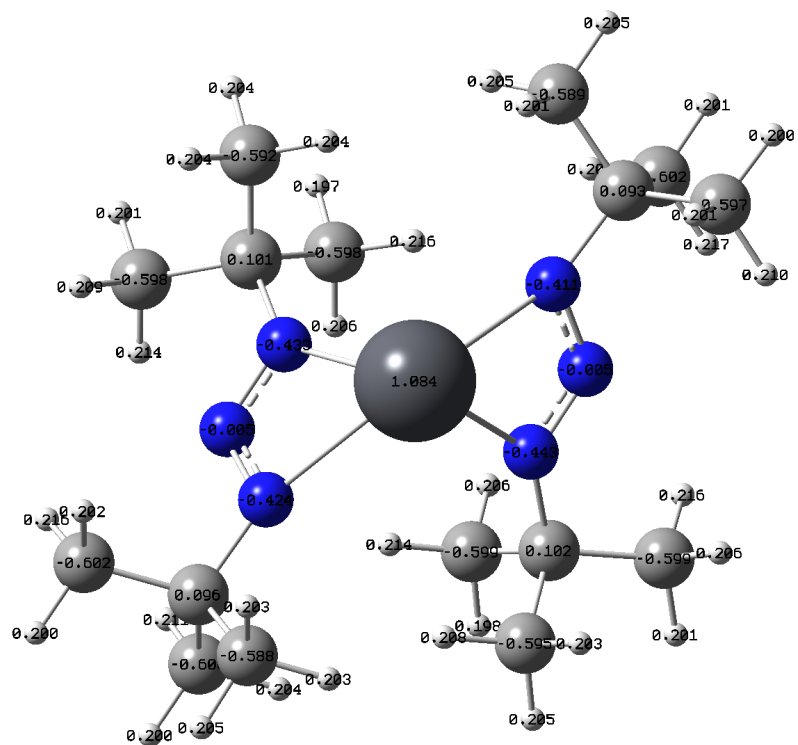


Figure S22: NBO charges for 3.